Evaluation of nuclear reaction cross sections for optimization of production of the important non-standard positron emitting radionuclide ^{89}Zr using proton and deuteron induced reactions on ^{89}Y target

N. Amjed [a,1], A. M. Wajid [a], N. Ahmad [a], M. Ishaq[b], M. N. Aslam[c], M. Hussain[d], S. M. Qaim[e]

[a] Department of Physics, Division of Science and Technology, University of Education, Lahore, Pakistan

[b] Applied Physics Division, National Centre for Physics, Islamabad, Pakistan.

[c] Department of Physics, COMSATS University Islamabad, Lahore Campus, Lahore, 54000, Pakistan.

[d] Department of Physics, Government College University Lahore, Lahore 54000, Pakistan

[e] Institut für Neurowissenschaften und Medizin, INM-5: Nuklearchemie, Forschungszentrum Jülich GmbH, D-52425 Jülich, Germany.

Abstract: ^{89}Zr ($T_{1/2}$ = 3.27 d) is an important β^+-emitting radionuclide of zirconium used in immuno PET. The excitation functions of the ^{89}Y(d,2n)^{89}Zr and ^{89}Y(p,n)^{89}Zr reactions were analyzed to deduce the optimum conditions for the high purity production of ^{89}Zr. The nuclear model codes ALICE-IPPE, EMPIRE 3.2 and TALYS 1.9 were used to check the consistency and reliability of the experimental data. A polynomial fit to the chosen data for each reaction gave the excitation function, which was then used for the integral yield calculation of the product. The amount of the major radioactive impurity ^{88}Zr was precisely analyzed for both the proton and the deuteron induced reactions on the ^{89}Y target.

Keywords:

Non-standard positron emitter zirconium-89 for immuno PET
Proton and deuteron induced reactions on ^{89}Y
Nuclear model analysis
Evaluated nuclear data
Thick target yield of ^{89}Zr

Highlights;

- Evaluation of ^{89}Y(d,2n)^{89}Zr and ^{89}Y(p,n)^{89}Zr reactions.
- Detailed nuclear model calculations (ALICE, TALYS and EMPIRE) and polynomial fitting of the selected data.
- Estimation of integral yield and impurity level in the production of ^{89}Zr.
- Comparison of production rates of ^{89}Zr in proton and deuteron induced reactions.

[1] Corresponding author.
E-mail address: noumanamjad@ue.edu.pk (N. Amjed)
noumanamjad@yahoo.co
Phone No: +923216026570

1 Introduction

Positron emission tomography (PET) has become a well-developed imaging modality. PET is usually performed using the conventional or so called "standard" short-lived positron emitters of organic nature, e.g. ^{18}F ($T_{1/2}$=110 min), ^{11}C ($T_{1/2}$=20.36 min) and ^{15}O ($T_{1/2}$=2 min) or metallic radionuclides, e.g. ^{38}K ($T_{1/2}$=7.5 min), ^{68}Ga ($T_{1/2}$=1.1 h), ^{82}Rb ($T_{1/2}$=1.3 min), etc. However, to study slow metabolic processes, like labelling of proteins, peptides and monoclonal antibodies (mAb), these short-lived nuclides are not very successful. Instead, longer lived positron emitting radionuclides are required to study slow metabolic process using PET. Several non-conventional termed as "non-standard" positron emitters have been developed, e.g. ^{124}I (4.18d), ^{64}Cu (12.7 h), ^{89}Zr (3.27 d), etc. to study the said slow metabolic processes (Qaim, 2011, 2012; Qaim et al., 2019). Out of those ^{89}Zr is an important non-standard positron emitter. On account of its suitable decay characteristics (Table 1) and chemical properties, several groups have been developing and using it to study slow biological processes (Verel et al., 2003; Zhang et al., 2011). ^{89}Zr is also used in immuno PET to treat breast cancer and ovary cancer (Cai et al., 2008; Bhattacharyya et al., 2013). It is applied in PET studies for the detection of lymph nodes metastases in head and neck cancer patients, and to analyze the antigen and antibodies interaction (Borjesson et al., 2006). PET using ^{89}Zr gives better spatial resolution as compared to CT and MRI (Link et al., 1986; Mendler et al., 2015). On the other hand, ^{89}Zr is used to study the tumor location and radiation dose monitoring of the cancer patient before immunotherapy, where ^{89}Zr is used as a PET surrogate radioisotope for scouting biodistribution of the therapeutic radionuclides, e.g. ^{90}Y and ^{177}Lu (Perk et al., 2005).

^{89}Zr has two isomeric states: ^{89m}Zr (metastable state with a half-life of 4.18 min) and ^{89g}Zr (ground state with a half-life of 3.27 d) (Table 1). ^{89}Zr can be effectively produced using the deuteron and proton induced reactions on ^{89}Y, namely ^{89}Y(d,2n)^{89}Zr and ^{89}Y(p,n)^{89}Zr. It can also be produced using alpha particle induced reactions on Sr isotopes, namely ^{86}Sr(α,n)^{89}Zr, ^{87}Sr(α,2n)^{89}Zr and ^{88}Sr(α,3n)^{89}Zr. But alpha induced reactions give lower rate of production with higher level of impurity and they also need high energy cyclotrons because of their higher thresholds. Therefore, alpha reactions are less suitable for the on-site (within the hospital) cyclotron production of ^{89}Zr. Because of the higher rate of production and low energy beam requirement, the proton and deuteron induced reactions on ^{89}Y are of considerable importance for the high-purity production of ^{89}Zr (Meijs et al., 1994; Holland et al. 2009; Tang et al., 2016; Link et al., 2017).

Thus, the specific aim of the present work was to evaluate the ^{89}Y(p,n)^{89}Zr and ^{89}Y(d,2n)^{89}Zr reactions for the production of ^{89}Zr. Since ^{88}Zr is also produced as the major radioactive impurity, via the reactions ^{89}Y(p,2n)^{88}Zr and ^{89}Y(d,3n)^{88}Zr, respectively, it should also be evaluated. While this work was being completed and our manuscript was in preparation, an evaluation of the two reactions for the production of ^{89}Zr, performed under a coordinated Research Project (CRP) of the IAEA, appeared in print (Tárkányi et al., 2019) The evaluation methodology used in that work, was, however, different than in our work. Those authors used a statistical approach to select the concordant set of experimental data and then a pade fitting was done to obtain the recommended excitation function. We used a theory-aided procedure to select

the data and then the fitting was performed by a polynomial function. We therefore considered it important and interesting to compare our results with those reported in the IAEA evaluation, discussing the agreement or disagreement, if any. On the other hand, it should be mentioned, that no evaluation of the impurity-producing reactions was presented in the CRP report (Tárkányi et al., 2019). From our study on those reactions, however, it should be possible to estimate the level of the ^{88}Zr impurity in the production of ^{89}Zr using protons or deuterons over various energy ranges within the ^{89}Y target.

2. Compilation and normalization of data, nuclear model calculations and evaluation methodology

2.1. Compilation and normalization

At first cross section data for the formation of ^{89}Zr and ^{88}Zr via protons and deuterons reactions on ^{89}Y were compiled. The experiments done on the reactions ^{89}Y(d,2n)^{89}Zr, ^{89}Y(p,n)^{89}Zr, ^{89}Y(d,3n)^{88}Zr and ^{89}Y(p,2n)^{88}Zr, their Q-values, thresholds and the references are given in Table 2.

All the reported experimental data were checked against the latest values of decay data (NuDat 2.7) and monitor reaction cross sections. Normalization factors were employed for the difference in decay and monitor reactions (Tárkányi et al., 2001). Those normalized data were then treated further.

2.2. Calculations using ALICE-IPPE, EMPIRE 3.2 and TALYS 1.9

To check the behavior of the excitation function as well as the consistency and reliability of the experimental data, three nuclear model calculations were performed using the codes TALYS 1.9, EMPIRE 3.2 and ALICE-IPPE. To obtain as good as possible agreement between the theoretical and experimental excitation function, different input nuclear model parameters were adjusted within their recommended limits (cf. RIPL-3,); details are given in our earlier work (Amjed et al., 2016). Besides check of reliability of the existing experimental data, the calculations helped to obtain the excitation function over energy regions where no experimental data were available.

ALICE code was introduced by Blann, which was later given the name ALICE-91 with some improvements and finally a few researchers at Obninsk presented a modified version named ALICE-IPPE (Dityuk et al., 1998). We made use of that code, which is based on Weisskopf-Ewing formalism. It does not calculate the isomeric states; therefore only total production cross sections were obtained.

The EMPIRE code has been essentially developed to analyse the nuclear reaction mechanisms. Due to the flexibility of models on the basis of incident particles its results come mostly very close to the experimental data. In EMPIRE calculations, optical model potentials (OMPs) of Morillon and Romain (2007) were used for the proton, and those of Perey and Perey (1963) for the deuteron.

TALYS is another professional nuclear model code used for nuclear reactions over a wide range of mass and energies (Koning and Rochman, 2012). For proton and deuteron the optical model potentials (OMPs) by Koning and Delaroche (2003) and by Bojowald et al, (1988), respectively, were used.

2.3. Evaluation methodology

The evaluation methodology was based on the theory-aided treatment of experimental data as discussed in a few previous articles (Aslam et al., 2010; Hussain et al., 2010; Sudár et al., 2002; Amjed et al., 2016). This involved two steps: (a) nuclear model calculation to ascertain consistency in the data, (b) fitting of the selected data by a polynomial function. Thus, at first, we calculated the ratio of experimental cross section to model calculation (that is $\sigma_{exp.}/\sigma$) for one of the three codes mentioned above. The ratio was then plotted against the energy range of experimental data, and a polynomial fitting was done, whereby the data showed the data that showed deviation three times greater than the standard deviation were eliminated. The remaining data were again fitted with a polynomial. The evaluated cross section $\sigma_{evaluated}$ was derived from the energy dependent normalization factor f(E) and the model calculated cross section $\sigma_{model}(E)$, such that

$$\sigma_{evaluated} = f(E)\, \sigma_{model}(E)$$

The weighting of the experimental uncertainties was also considered in the polynomial fitting and the fitted cross sections were calculated with 95% upper/lower confidence limits. The same steps were repeated for the other two model calculations as well. The best fit was obtained by taking an average of all the three normalized model calculations along with 95% confidence limits. Those data are called recommended cross sections.

It should be mentioned that for a few nuclear reactions we could not obtain a reasonable agreement between the experimental data and the model calculation, despite the permissible variation in the input parameters, in those cases we therefore performed only a polynomial fitting through the experimental data.

3. Evaluation of production data of ^{89}Zr using ^{89}Y as target

3.1 ^{89}Y(d,2n)^{89}Zr reaction

The database of this reaction is fairly strong; eight authors have reported experimental values for this reaction (Table 2). The reported values by Manenti et al. (2019), Lebeda et al. (2015), Baron et al. (1963), Uddin et al. (2005) and West et al. (1993) are consistent with each other and also with the results of nuclear model codes. Only the experimental values by Bissem et al. (1980) are

a bit lower than the other reported values in the literature. The values reported by La Gamma et al. (1973) and Degering et al. (1988) are lower than the other experiments; this difference cannot be adjusted with their reported monitor reaction and decay data, so those values were deselected in further evaluation. For each set of experimental data, the above mentioned normalization procedure was adopted on the basis of decay data and monitor reactions.

The results of nuclear model calculations (using ALICE-IPPE, TALYS 1.9 and EMPIRE 3.2) along with all normalized experimental data are shown in Figure 1. The general trends of all three model calculations and experimental data are similar. ALICE overestimates the excitation function in the peak region and TALYS shows better consistency but with a slight energy shift. EMPIRE shows the best consistency with the experimental data in all regions. It is known that, in general, the deuteron induced reactions are not well reproduced by model calculations.

Using the above-mentioned theory-aided evaluation methodology, the ratios of experimental and calculated cross section by EMPIRE 3.2 were plotted as a function of deuteron energy (Figure 2) and a polynomial fit with 95% confidence limits was obtained. Then by deselecting the values beyond 3σ limit, the polynomial fit was repeated again. These fitted values were multiplied with EMPIRE results to produce the normalized EMPIRE values. The same method was used to obtain the normalized values by TALYS 1.9 and ALICE-IPPE. All three normalized values were then averaged to obtain the recommended cross section. The recommended curve with 95% confidence limits and with selected experimental data is shown in Figure 3; where encircled points show the deselected values. Numerical values of the recommend fit with 95% confidence limits are given in Table 3.

3.2 ^{89}Y(p,n)^{89}Zr reaction

In literature the ^{89}Y(p,n)^{89}Zr reaction has been described as the most favorable route for the production of ^{89}Zr. The database of this reaction is quite strong; in total seventeen groups reported experimental data for this reaction (Table 2). Normalized experimental cross sections for all the literature experiments along with the results of nuclear model calculations (using ALICE-IPPE, TALYS 1.9 and EMPIRE 3.2) are shown in Figure 4. The reported values by Birattari et al. (1988) and Saha et al. (1966) are too high whereas the single point reported by Blosser and Handley (1955) is very low. These scattered measurements cannot be normalized for decay data and monitor reaction, so these values were deselected and not used in further evaluation process.

All the other reported experiments agreed well with each other the values reported by Satheesh et al. (2011) and Delaunay-Olkowsky et al. (1963). The literature values by Satheesh et al. (2011) show slight energy shift towards the lower energy whereas the single point reported by Delaunay-Olkowsky et al. (1963) is slightly lower than the other reported literature values. The reported data by Steyn et al. (2011) and Levkovskij (1991) were normalized by 3% and 18%, respectively, for their difference of monitor reaction cross section (Qaim et al., 2014).

Theoretical results by EMPIRE 3.2 and TALYS 1.9 show good agreement with the experimental data whereas the predictions of ALICE-IPPE are slightly higher than those of and the other two model calculations. The overall trends of theoretical and experimental excitation functions are quite similar. The above-mentioned evaluation methodology was employed to generate the recommended fit. The recommended curve with 95% confidence limits, along with the selected experimental data, is shown in Figure 5, and the numerical values are given in Table 4.

4 Comparison of our evaluation with earlier evaluation of ^{89}Zr production data

As mentioned in the introduction, besides our work the two production routes of ^{89}Zr, namely ^{89}Y(d,2n), ^{89}Y(p,n) were also evaluated under a recent Coordinated Research Project (CRP) of the IAEA (Tárkányi et al., 2019). In that work the selections of concordant experimental data was based on purely statistical consideration and a PADE fitting of the selected experimental data was done with region wise percentage uncertainty.

The present work gives a more detailed evaluation because the selection of experimental data is based on of three nuclear model calculations, i.e. ALICE-IPPE, TALYS 1.9 and EMPIRE 3.2 and the recommended data were generated by a polynomial fitting with 95% confidence limits. Our choice (or rejection) of experimental data is thus based on a more scientific and rigorous analysis. The results of the two evaluations are, however, in agreement within the 95% confidence limits. This is because the recommended data in both the evaluations are based on fitting of a large number of concordant results.

5 Data for formation of impurities

During the use of radionuclides, impurities can cause the problems of low spatial resolution and higher radiation dose to the patient. Therefore, high purity production of the medical radionuclide is mandatory. In the production of ^{89}Zr, impurities other than the Zr isotopes can be separated chemically, but in both ^{89}Y(d,2n)^{89}Zr and ^{89}Y(p,n)^{89}Zr reactions, the longer lived ^{88}Zr ($T_{1/2}$ = 83.4 d) is the only radionuclidic impurity that cannot be separated chemically. This impurity can be avoided by the optimization of the process, i.e. by a careful selection of the energy range where the rate of production of the desired radionuclide is good and the level of the radioisotopic impurity is low (Qaim, 1982, 2001). So, to study the said radionuclidic impurity two further reactions were analyzed.

In the deuteron induced production of ^{89}Zr the radioisotope ^{88}Zr is formed via the ^{89}Y(d,3n)^{88}Zr reaction. Normalized cross sections from the literature along with the default TALYS calculation are shown in Figure 6. All the experimental values are consistent with each other within the limits of their uncertainties, but the TALYS overestimates the cross section up to 29 MeV and then underestimates after 32 MeV. The threshold and to some extent the overall trend of the theory and the experiment are similar. However, a better agreement could not be obtained even by varying the input parameters (within their limits) and of the model calculation. As mentioned in the section 2.3 above, we therefore relied on the experimental data. A polynomial fit to the normalized cross sections was performed to generate the recommended cross sections of the ^{89}Y(d,3n)^{88}Zr reaction (Figure 6).

In the proton induced production of ^{89}Zr, ^{88}Zr ($T_{1/2}$ = 83.4 d) is produced via the ^{89}Y(p,2n)^{88}Zr reaction. All normalized reported literature values along with the results of default TALYS calculations are shown in Figure 7. All the literature values are consistent with each other within the limits of their uncertainties. The TALYS calculation shows some deviations. Therefore, we relied again on the experimental data. A polynomial fit of the selected normalized literature data was used to generate the recommended cross sections of this reaction (Figure 7).

6 Calculation and comparison of thick target yield

From the recommended excitation functions the thick target yields (Amjed et al., 2013) of ^{89}Zr were calculated using the standard formula (Qaim, 1982), assuming a beam current of 1 μA and an irradiation time of 1 h (Otuka and Takacs, 2015). Those yields serve as reference for the maximum value that can be achieved in any experiment using the suggested energy range. The calculated thick target yields for both ^{89}Y(d,2n)^{89}Zr and^{89}Y(p,n)^{89}Zr are given in Figures 8 and 9, respectively. To make a comprehensive impurity analysis, thick target yields of the corresponding impurity reactions, ^{89}Y(d,3n)^{88}Zr and ^{89}Y(p,2n)^{88}Zr, were also calculated and the results are compared in Figures 8 and 9.

6.1 Thick target yields of ^{89}Y(d,2n)^{89}Zr and ^{89}Y(d,3n)^{88}Zr reactions

Besides the calculated integral yields of the ^{89}Y(d,2n)^{89}Zr and ^{89}Y(d,3n)^{88}Zr reactions, shown in Figure 8, a single yield value reported by Dmitriev et al. (1983) at 22 MeV for the ^{89}Y(d,2n)^{89}Zr reaction is also given, It is lower than our calculated thick target yield. A comparison of ^{89}Zr and ^{88}Zr yields shows that up to 17 MeV 100% pure ^{89}Zr can be achieved with a yield value of 74 MBq/μAh. If a higher yield is desired, one can select the energy window of 30→17 MeV, which would give 122 MBq/μAh of ^{89}Zr; however, with 3% of ^{88}Zr impurity.

It is also interesting to compare the theoretical yields with the results obtained in real high-current production runs. Zweit et al. (1991) reported a ^{89}Zr yield of 67 MBq/ μAh of ^{89}Y target over the energy range E_d = 16→7 MeV at a beam current of 3-5 μA. The experimental and

theoretical values are thus comparable. In another experiment, Tang et al. (2016) obtained a ^{89}Zr yield of 58%±5 MBq/μAh in the irradiation of ^{89}Y with 13 MeV deuterons at a beam current of 10-15 μA. This experimental value is almost double of the theoretical value and is probably in error.

6. 2 Thick target yields of ^{89}Y(p,n)^{89}Zr and ^{89}Y(p,2n)^{88}Zr reactions

The ^{89}Y(p,n)^{89}Zr reaction is considered as the method of choice for high quality production of the radionuclide ^{89}Zr. Using the recommended cross section data the thick target yields of the ^{89}Y(p,n)^{89}Zr and ^{89}Y(p,2n)^{88}Zr reactions were calculated; these values are shown in Figure 9, along with the reported literature values by Dmitriev (1986) and Dmitriev and Molin (1982). The reported values by Dmitriev (1986) are in agreement with our calculated values up to 18 MeV; thereafter their values are higher than the calculated values. Our calculated yield values are also higher than the single experimental value reported by Dmitriev and Molin (1982).

If we compare the rate of production of the desired product ^{89}Zr and that of the impurity ^{88}Zr, it is clearly seen from Figure 9 that the contribution of the longer lived ^{88}Zr impurity starts rising from 14 MeV onwards. Omara et al. (2009) have reported 58 MBq/μAh of ^{89}Zr for 14→9 MeV, whereas our calculated yield for the same region is 63 MBq/μAh but with 0.36% contribution of near radioisotopic impurity ^{88}Zr. So, if we select the energy range 13→9 MeV, it gives 100% pure ^{89}Zr with 0% of the radioisotopic impurity ^{88}Zr. The calculated integral yield (this work) of ^{89}Zr over this energy is 50.4 MBq/μAh.

In contrast to the ^{89}Y(d,2n)^{89}Zr reaction, the ^{89}Y(p,n)^{89}Zr reaction has been extensively used for the production of ^{89}Zr and its practical yields of about 45±2 MBq/μAh have been reported in high-current irradiations with proton energy of 14 MeV(Holland et al., 2009; Meijs et al., 1994; Tang et al., 2016). At a proton energy of 11 MeV the yield of ^{89}Zr amounted to 23±2 MBq/μAh (Link et al., 2017). All those values are slightly lower than the theoretical values but this is always expected in a high-current irradiation. An important corollary is that the data appear to be in good shape and production technology is optimized.

7. Comparison of production routes and new perspectives

The optimized energy ranges for high production rate of ^{89}Zr with minimum level of the radionuclidic impurity ^{88}Zr, deduced from our recommended cross sections, are summarized in Table 5. Out of the two evaluated nuclear processes, the deuteron induced reaction gives a relatively low production rate of up to 15 MeV. Beyond this energy, the yield increases with the increasing deuteron energy but the level of the radionuclidic impurity also increases. On the other hand, the proton induced reaction gives moderate yield with negligible radionuclidic impurity. Moreover it facilitates the production of ^{89}Zr at low energy cyclotrons.

For the $^{89}Y(p,n)^{89}Zr$ reaction our suggested optimized energy range is E_p = 13→9 MeV. Using this production route, high purity production of ^{89}Zr is already being performed at low energy cyclotrons in the vicinity of hospitals. The deuteron energy available at those machines is much lower than the proton energy.

Since both of the above mentioned reactions give relatively high rate of ^{89}Zr production, it is instructive to compare them; as shown in Figure 10. In the low energy region the rate of production of ^{89}Zr by the proton beam is higher as compared to the deuteron beam but beyond 22 MeV the deuteron beam gives higher production rate than the proton beam. Thus at low energy medical cyclotrons the proton induced reaction gives better rate of production than the deuteron induced reaction. Using high-current solid targets, experimental batch yields of GBq amounts of ^{89}Zr have been achieved via the (p,n) reaction and the technology is now being commercialized. In view of the increasing importance of ^{89}Zr, however, in recent years attempts are also underway to produce this radionuclide at medical cyclotrons for in-house use. Since at those cyclotrons generally only liquid and gaseous targets are available (to produce ^{18}F and ^{11}C), a new type of solution target has been developed in which a $Y(NO_3)_3$ solution is irradiated. This introduces an extra burden of removing radiation-induced chemical products, and the batch yield of ^{89}Zr also amounts to only about 15% of the yield from a solid target. Nonetheless, it has been shown (Pandey et al., 2016) that the yield and purity of ^{89}Zr are sufficient for local use. As far as nuclear data work is concerned, the importance of well-evaluated accurate data near the reaction threshold cannot be overemphasized.

7 Conclusion

In this work, for the production of the positron emitter ^{89}Zr, two main routes, namely $^{89}Y(d,2n)^{89}Zr$ and $^{89}Y(p,n)^{89}Zr$, were evaluated and their recommended cross sections were generated. The corresponding impurity reactions were also evaluated. The $^{89}Y(p,n)^{89}Zr$ reaction is the method of choice. Using this reaction ^{89}Zr can be produced at low energy cyclotrons in the vicinity of the hospitals. In fact this method is already in use in many laboratories. Our evaluated data should provide a better base for calculation of the theoretical yield, especially near the threshold of the reaction, which is important with regard to the use of a solution target for production purposes. The $^{89}Y(d,2n)^{89}Zr$ reaction is also a favorable method but high energy cyclotron requirement makes this method a less convenient choice.

Acknowledgments

N. Amjed would like to thank the Higher Education Commission of Pakistan (HEC) for the financial assistance. The work was done in the frame of HEC; NRPU project No. 9746.

References:

Albert, R. (1959). (p,n) cross section and proton optical-model parameters in the 4- to 5.5-MeV energy region. *Phys. Rev., 115,* 925-927.

Amjed, N., Hussain, M., Aslam, M. N., Tárkányi, F., Qaim, S. M. (2016). Evaluation of nuclear reaction cross sections for optimization of production of the emerging diagnostic radionuclide ^{55}Co. *Appl. Radiat. Isot., 108,* 38-48.

Amjed, N., Tárkányi, F., Ditrói, F., Takács, S., Yuki, H. (2013). Activation cross-sections of deuteron induced reactions of natural Ni up to 40 MeV. *Appl. Radiat. Isot.*, 82, 87-99.

Aslam, M. N., Sudár, S., Hussain, M., Malik, A.A., Shah, H. A., Qaim, S. M. (2010). Evaluation of excitation functions of proton and deuteron induced reactions on enriched tellurium isotopes with special relevance to the production of iodine-124. *Appl. Radiat. Isot., 68,* 1760-1773.

Baron, N., Cohen, B, L. (1963). Activation cross-section survey of deuteron-induced reactions. *Phys. Rev., 129(6),* 2636-2642.

Bhattacharyya, S., Kurdziel, K., Wei, L., Riffle, L., Kaur, G., Hill, G. C., Jacobs P. M., Tatum J. L., Doroshow J. H., Kalen, J. D. (2013). Zirconium-89 labeled panitumumab: a potential immuno-PET probe for HER1-expressing carcinomas. *Nuclear Medicine and Biology*, *40*(4), 451-457.

Birattari, C., Gadioli, E., Gadioli Erba, E., Strini, M. G., Strini, G., Tagliaferri, G. (1973). Pre-equilibrium processes in (p,n) reactions. *Nuclear Physics, A201*, 579-592.

Bissem, H. H., Georgi, R., Scobel, W., Ernst, J., Kaba, M., Rao, J. R., Strohe, H. (1980). Entrance and exit channel phenomena in d- and He^3- induced preequilibrium decay. *Phys. Rev., C 22(4),* 1468-1484.

Blaser, J. P., Boehm, F., Marmer, P., Scherrer, P. (1951). Excitation funtions and cross section of the (p,n) reaction. *Helvetica Physica Acta, 24(5),* 441-464.

Blosser, H. G., Handley, T. H. (1955). Survey of (p,n) reactions at 12 MeV. *Phys. Rev., 100(5),* 1340-1344.

Bojowald, J., Machner, H., Nann, H., Oelert, W., Rogge, M., Turek, P. (1988). Elastic deuteron scattering and optical model parameters at energies upto100 MeV. *Phys. Rev., C 38,* 1153-1163.

Borjesson, P. K., Jauw, Y. W., Boellaard, R., De Bree, R., Comans, E. F., Roos, J. C., Castelijns, J.A., Vosjan, M.J., Kummer, J.A., Leemans, C.R., Lammertsma, A. A. (2006). Performance of immuno–positron emission tomography with zirconium-89-labeled chimeric monoclonal antibody U36 in the detection of lymph node metastases in head and neck cancer patients. *Clinical Cancer Research, 12*(7), 2133-2140.

Cai W, Niu G, Chen X. (2008). Multimodality imaging of the HER-kinase axis in cancer. *Eur. J. Nucl. Med. Mol. Imaging., 35*, 186-208.

Caretto, A. A., Wing E.O. (1959). Interaction of yttrium with protons of energy between 60 and 240 MeV. *Phys. Rev., 115*, 1238-1242.

Degering, D., Unterricker, S., Stolz, W. (1988). Excitation function of the ^{89}Y(d,2n)^{89}Zr reaction. J. *Radioanal. Nucl. Chem., 127(1)*, 7-11.

Delaunay-Olkowsky, J., Strohal, P., Cindro, N. (1963). Total reaction cross sections of proton induced reactions. *Nuclear Physics, 47*, 266-272.

Dityuk, A. I., Konobeyev, A. Y., Lunev, V. P., Shubin, Y. N. (1998). New advanced version of computer code ALICE-IPPE . IAEA,Vienna. *Report.INDC(CCP)-410*.

Dmitriev, P. P. (1986). Radionuclide yield in reactions with protons, deuterons, alpha particles and helium-3: Handbook. IAEA,Vienna. *Report.INDC(CCP)-263*.

Dmitriev, P. P., Krasnov, N. N., Molin, G. A. (1983). Yields of radioactive nuclides formed by bombardment of a thick target with 22-MeV deuterons. IAEA,Vienna. *Report.INDC(CCP)-210.*

Dmitriev, P. P., Molin, G. A. (1982). Radionuclide yields for thick targets at 22 MeV proton energy . IAEA,Vienna. *Report.INDC(CCP)-188*.

Holland, J. P., Phill, D., Sheh, Y., Lewis, J. S. (2009). Standardized methods for the production of high specific acitivity ^{89}Zr. *Nucl. Med. Bio., 36(7)*, 729-739

Hussain, M., Sudár, S., Aslam, M. N., Malik, A. A., Ahmad, R., Qaim, S. M. (2010). Evaluation of charged particle induced reaction cross section data for production of the important therapeutic radionuclide ^{186}Re. *Radiochim. Acta, 98*, 385-395.

Johnson, C. H., Kernell, R. L. (1968). The ^{89}Y(p,n)^{89}Zr cross section near the first two analogue resonances. *Nuclear Phys. A, 107(1)*, 21-34.

Khandaker, M. U., Kim, K., Lee, M. W., Kim, K. S., Kim, G., Otuka, N. (2012). Investigations of ^{89}Y(p,x)^{86,88,89g}Zr, $^{86m+g,87g,87m,88g}$Y, ^{85g}Sr, and ^{84g}Rb nuclear processes up to 42 MeV. *Nucl. Instrum. Methods, B 271*, 72–81.

Koning, A. J., Delaroche, J. P. (2003). Local and global nucleon optical models from 1 keV to 200 MeV. *Nucl.Phys., A 713*, 231-310.

Koning, A. J., & Rochman, D. (2012). Modern nuclear data evaluation with the TALYS code system. *Nuclear Data Sheets*, 113(12), 2841-2934.

La Gamma, A. M., Nassiff, S. J. (1973). Excitation function for deuteron induced reactions on ^{89}Y. *Radiochim. Acta, 19*, 161-165.

Lebeda, O., Stursa, J., Ralis, J. (2015). Experimental cross-sections of deuteron-induced reactions on ^{89}Y up to 20 MeV; comparison of ^{nat}Ti(d,x)^{48}V and ^{27}Al(d,x)^{24}Na monitor reactions. *Nuclear Instrum. Methods B, 360*, 118-128.

Levkovskij, V. N. (1991). Cross Section of medium mass nuclide activation (A= 40-100) by medium energy proton and alpha particles (E = 10-50 MeV). *Inter-Vesi*,Moscow.

Link, J. M., Krohn, K. A., Eary, J. F., Kishore, R., Lewellen, T. K., Johnson, M. W., Badger, C. C., Richter, K. Y., Nelp, W. B. (1986). ^{89}Zr for antibody labeling and positron emission tomography. *Label. Compds. Radiopharm., 23*, 1297-1298.

Link, J. M., Krohn, K. A., O' Hara, M. J. (2017). A simple thick target for production of ^{89}Zr using 11 MeV cyclotron. *Appl. Radiat. Isot.*, 122, 211-214.

Manenti, S., Groppi, F., Haddad, F. (2019). New excitation functions measurement of nuclear reactions induced by deuteron beams on yttrium with particular reference to the production of ^{89}Zr. *Nuclear Instrum. Methods, B 458*, 57-60.

McFadden, L., Satchler, G. R. (1966). Optical model analysis of the scattering of 24.7 MeV α-particles. *Nucl.Phys., 84*, 177-200.

Meijs, W. E., Herscheid, J. D., Haisma, H. J., Wijbrandts, R., van Langevelde, F., Van Leuffen, P. J., Mooy, R. Pinedo, H. M. (1994). Production of highly pure no-carrier added ^{89}Zr for the labeling of antibodies with a positron emitter. *Appl. Radiat. Isot., 45*, 1143-1147.

Mendler, C. T., Gehring, T., Wester, H. J., Schwaiger, M., Skerra, A. (2015). ^{89}Zr-labeled versus ^{124}I-labeled αHER2 fab with optimized plasma half-life for high-contrast tumor imaging in vivo. *J. Nucl Med*, 56(7), 1112-1118.

Michel, R., Bodemann, R., Busemann, H., Daunke, R., Gloris, M., Lange, H. J., Filges, D. (1997). Cross sections for the production of residual nuclides by low- and medium-energy protons from the target elements C, N, 0, Mg, Al, Si, Ca, Ti, V, Mn, Fe, Co, Ni, Cu, Sr, Y, Zr, Nb, Ba and Au. *Nucl. Instrum. Methods., B 129*, 153-193.

Morillon, B., Romain, P. (2007). Bound single-particle states and scattering of nucleons on spherical nuclei with a global optical model. *Phys. Rev. C 76, 044601–044611.*

Mustafa, M. G., West , H. I., Brien, O., Lanier, R. G., Benhamou, M., Tamura, T. (1988). Measurements and direct-reaction-plus-Hauser-Feshbach analysis of ^{89}Y(p,n)^{89}Zr, ^{89}Y(p,2n)^{88}Zr and ^{89}Y(p,pn)^{88}Y reactions up to 40 MeV. *Phys. Rev., C 38*, 1624-1637.

NuDat 2.7. Data source :National Nuclear Data Center, Brookhaven National Laboratory,based on ENSDF and the Nuclear Wallet Carlds,available from ⟨http://www.nndc.bnl.gov/nudat2⟩.

Omara , H. M., Hassan, K. F., Kandil S. A., Hegazy F. E., Saleh Z. A. (2009). Proton induced reactions on ^{89}Y with particular reference to the production of the medically interesting radionuclide ^{89}Zr. *Radiochim. Acta, 97*, 467-471.

Otuka, N., Takacs, S., 2015. Definitions of radioisotope thick target yields. *Radiochim. Acta*, 103, 1-6

Pandey, M. K., Bansal, A., Engelbrecht, H. P., Byrne, J. F., Packard, A. B., DeGrado, T. R. (2016). Improved production and processing of ^{89}Zr using a solution target. *Nuclear Medicine and Biology*, *43*(1), 97-100.

Perey, C. M., Perey, F. G. (1963). Deuteron optical model analysis in the range of 11 to 27 MeV. *Phys. Rev., 132*, 755-773.

Perk, L. R., Visser, G. W., Vosjan, M. J., Stigter-van Walsum, M., Tijink, B. M., Leemans, C. R., Van Dongen, G.A. (2005). ^{89}Zr as a PET surrogate radioisotope for scouting biodistribution of the therapeutic radiometals ^{90}Y and ^{177}Lu in tumor-bearing nude mice after coupling to the internalizing antibody cetuximab. *J. Nucl. Med., 46*, 1898-1906.

Qaim, S. M. (1982). Nuclear data relevant to cyclotron produced short-lived medical radioisotopes. *Radiochim. Acta*, 147-162.

Qaim S. M. (2001). Nuclear data for medical applications: an overview. *Radiochim. Acta, 89*, 189–196.

Qaim S. M. (2011). Development of novel positron emitters for medical applications: nuclear and radiochemical aspects. *Radiochim. Acta, 99*, 611-625.

Qaim S. M. (2012). The present and future of medical radionuclide production. *Radiochim. Acta, 100*, 635-651.

Qaim S. M., Sudár, S., Scholten, B., Koning, A. J., Coenen, H. H., (2014). Evaluation of excitation functions of ^{100}Mo(p,d+pn)^{99}Mo and ^{100}Mo(p,2n)^{99m}Tc reactions: Estimation of long-lived Tc-impurity and its implication on the specific activity of cyclotron-produced ^{99m}Tc. *Appl. Radiat. Isot., 85*, 101-113.

Qaim, S. M., Scholten, B., Spahn, I., Nenmaier, B. (2019). Positron-emitting radionuclides for applications with special emphasis on their production methodologies for medical use. *Radiochim. Acta*, 107, 1011-1026.

RIPL-3 database, international Atomic Energy Agency, Vienna. Available from (www.ds-iaea.org/RIPL-3/).

Saha, G. B., Porile, N. T. (1966). (p, xn) and (p,pxn) reactions of Yttrium-89 with 5-85-MeV Protons. *Phys. Rev., 144(3)*, 962-971.

Satheesh, B., Musthafa, M. G. (2011). Nuclear isomers ^{90m,g}Zr, ^{89m,g}Zr, ^{89m,g}Y and ^{85m,g}Sr formed by bombardment of ^{89}Y with protons of energies from 4 to 40 MeV. *International Journal of Modern Physics E 20(10)*, 2119--2131.

Steyn, G. F., Vermeulen, C., Szelecsenyi, F., Kovacs, Z., Suzuki, K., Fukumura, T., Nagatsu, K. (2011). Excitation functions of proton induced reactions on ^{89}Y and ^{93}Nb with emphasis on the production of selected radio-zirconiums. *Journal of Korean Physics, 59(23),* 1991-1994.

Sudár, S., Cserpák, F., Qaim, S. M. (2002). Measurements and nuclear model calculations on proton induced reactions on ^{103}Rh upto 40 MeV: Evaluation of the excitation function of the ^{103}Rh(p,n)^{103}Pd reaction relevant to the production of the therapeutic radionuclide ^{103}Pd. *Appl. Radiat. Isot., 56*, 821-831.

Tang, Y., Li, S., Yang, Y., Chen, W., Wei, H., Wang, G., Yang, J., Liao, J., Luo, S., Luo, N. (2016). A simple and convenient method for production of ^{89}Zr with high purity. *Appl. Radiat. Isot., 118*, 326-330.

Tárkányi, F., Ditrói, F., Takács, S., Csikai, J., Mahunka, I., Uddin, M. S., Hagiwara, M., Baba, M., Ido, T., Hermanne, A., Sonck, M., Shubin, Yu., Sonck, M. (2005). Excitation functions for production of ^{88}Zr and ^{88}Y by proton and deuteron irradiation of Mo, Nb, Zr, and Y. In AIP Conference Proceedings (Vol. 769, No. 1, pp. 1658-1661). American Institute of Physics.

Tárkányi, F., Ignatyuk, A. V., Hermanne, A., Capote, R., Carlson, B. V., Engle, J. W., Verpelli, M., Kellett, M. A., Kibedi, T., Kim, G., N., Kondev, F. G., Hussain, M. (2019). Recommended nuclear data for medical radioisotope production: diagnostic positron emitters. *J. Radioanal. Nucl. Chem., 319*, 533-666.

Tárkányi, F., Takács, S., Gul, K., Hermanne, A., Mustafa, M. G., Nortier, M., Oblozinsky, P., Qaim, S. M., Scholten, B., Shubin, Y. N., Youxiang, Z. (2001). Charged particle cross-section data base for medical radioisotope production : diagnostic radioisotopes and monitor reactions. *IAEA-TECDOC-1211*, 49-97.

Uddin, M. S., Baba, M., Hagiwara, M., Tárkányi, F., Ditrói, F. (2007). Experimental determination of deuteron-induced activation cross sections of yttrium. *Radiochim. Acta, 95*, 187-192.

Uddin, M.S, Hagiwara, M., Baba, M., Tarkanyi, F., Ditroi, F. (2005). Experimental studies on excitation functions of the proton-induced activation reactions on yttrium. *Appl. Radiat. Isot., 63*, 367-374.

Verel, I., Visser, G. W., Boellaard, R., Stigter-van Walsum, M., Snow, G. B., Van Dongen, G. A. (2003). ^{89}Zr immuno-PET: comprehensive procedures for the production of ^{89}Zr-labeled monoclonal antibodies. *J. Nucl. Med., 44*(8), 1271-1281.

Wenrong, Z., Shen, Q. L., Weixiang Hanlin, Y. (1992). Investigation of ^{89}Y(p,n)^{89}Zr, ^{89}Y(p,2n)^{88}Zr and ^{89}Y(p,pn)^{88}Y reactions up to 22 MeV. *Chin. J. Nucl. Phys. (Beijing), 97(9)*, 467-471.

West, H. I., Brien, H. O., Lanier, R. G., Nagle, R. J., Mustafa, M. G., (1993). Measurements of the excitation functions of the isobaric chain ^{87}Y, ^{87m}Y, ^{87g}Y, and ^{87m}Sr. Some excitation

functions of proton and deuteron induced reactions on ^{89}Y. Prog: UC, Lawrence Radiat. Lab., Berkeley and Livermore, USA, 4(115738), 1.

Zhang, Y., Hong, H., & Cai, W. (2011). PET tracers based on Zirconium-89. *Current Radiopharmaceuticals*, *4*(2), 131-139.

Zweit, J., Downey, S., Sharma, H. L., 1991. Production of no-carrier-added zirconium-89 for Positron emission tomography. *Appl. Radiat. Isot.* 42, 199-201.

List of Figure Captions

Figure 1 All normalized experimental data, together with the results of nuclear model calculations (ALICE-IPPE, TALYS 1.9 and EMPIRE 3.2) for the ^{89}Y(d,2n)^{89}Zr reaction.

Figure 2 Ratio of experimental cross section to model calculation result by EMPIRE shown as a function of deuteron energy. The encircled data points are out of 3σ limits.

Figure 3 Selected experimental data and recommended fit for the ^{89}Y(d,2n)^{89}Zr reaction. Deselected points are encircled.

Figure 4 All normalized experimental data, together with the results of nuclear model calculations (ALICE-IPPE, TALYS 1.9 and EMPIRE 3.2) for the ^{89}Y(p,n)^{89}Zr reaction.

Figure 5 Recommended fit for the ^{89}Y(p,n)^{89}Zr reaction cross sections.

Figure 6 All normalized experimental cross section data with the results of TALYS 1.9 nuclear code and with recommended polynomial fit of the ^{89}Y(d,3n)^{88}Zr reaction cross sections.

Figure 7 All normalized experimental cross section data with the results of TALYS 1.9 nuclear code and with recommended polynomial fit of the ^{89}Y(p,2n)^{88}Zr reaction cross sections.

Figure 8 Calculated integral yield of the ^{89}Y(d,2n)^{89}Zr reaction along with a literature experimental yield value, and calculated integral yield of the impurity reaction ^{89}Y(d,3n)^{88}Zr.

Figure 9 Calculated integral yield of the ^{89}Y(p,n)^{89}Zr reaction along with literature experimental yield values, and calculated integral yield of the impurity reaction ^{89}Y(p,2n)^{88}Zr.

Figure 10 Comparison of thick target yields of ^{89}Zr from ^{89}Y(p,n)^{89}Zr and ^{89}Y(d,2n)^{89}Zr reactions.

Highlights;

- Evaluation of $^{89}Y(d,2n)^{89}Zr$ and $^{89}Y(p,n)^{89}Zr$ reactions.
- Detailed nuclear model calculations (ALICE, TALYS and EMPIRE) and polynomial fitting of the selected data.
- Estimation of integral yield and impurity level in the production of ^{89}Zr.
- Comparison of production rates of ^{89}Zr in proton and deuteron induced reactions.

Figure 1

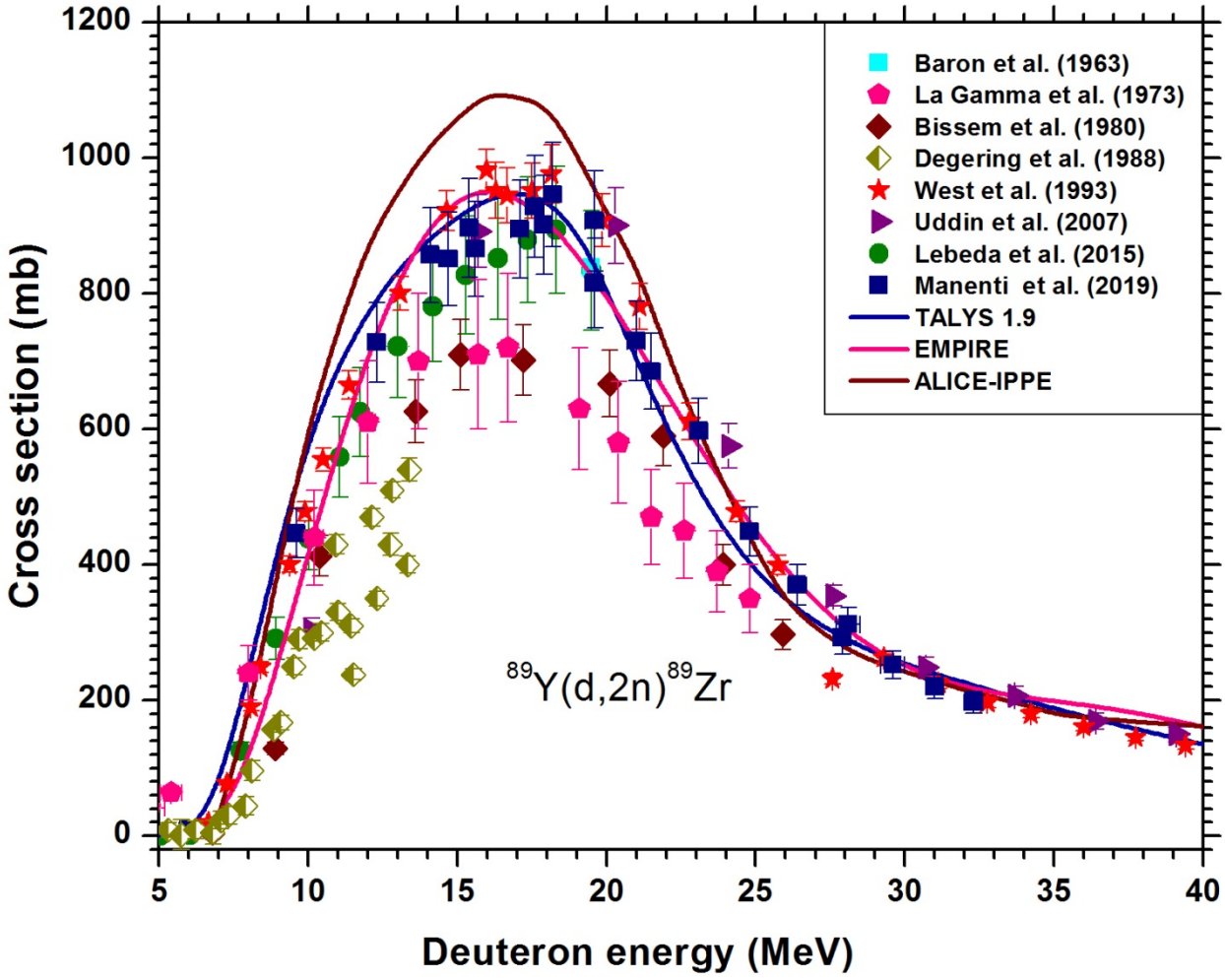
Cross section (mb)
Deuteron energy (MeV)
^{89}Y(d,2n)^{89}Zr
Baron et al. (1963)
La Gamma et al. (1973)
Bissem et al. (1980)
Degering et al. (1988)
West et al. (1993)
Uddin et al. (2007)
Lebeda et al. (2015)
Manenti et al. (2019)
TALYS 1.9
EMPIRE
ALICE-IPPE

Figure 2

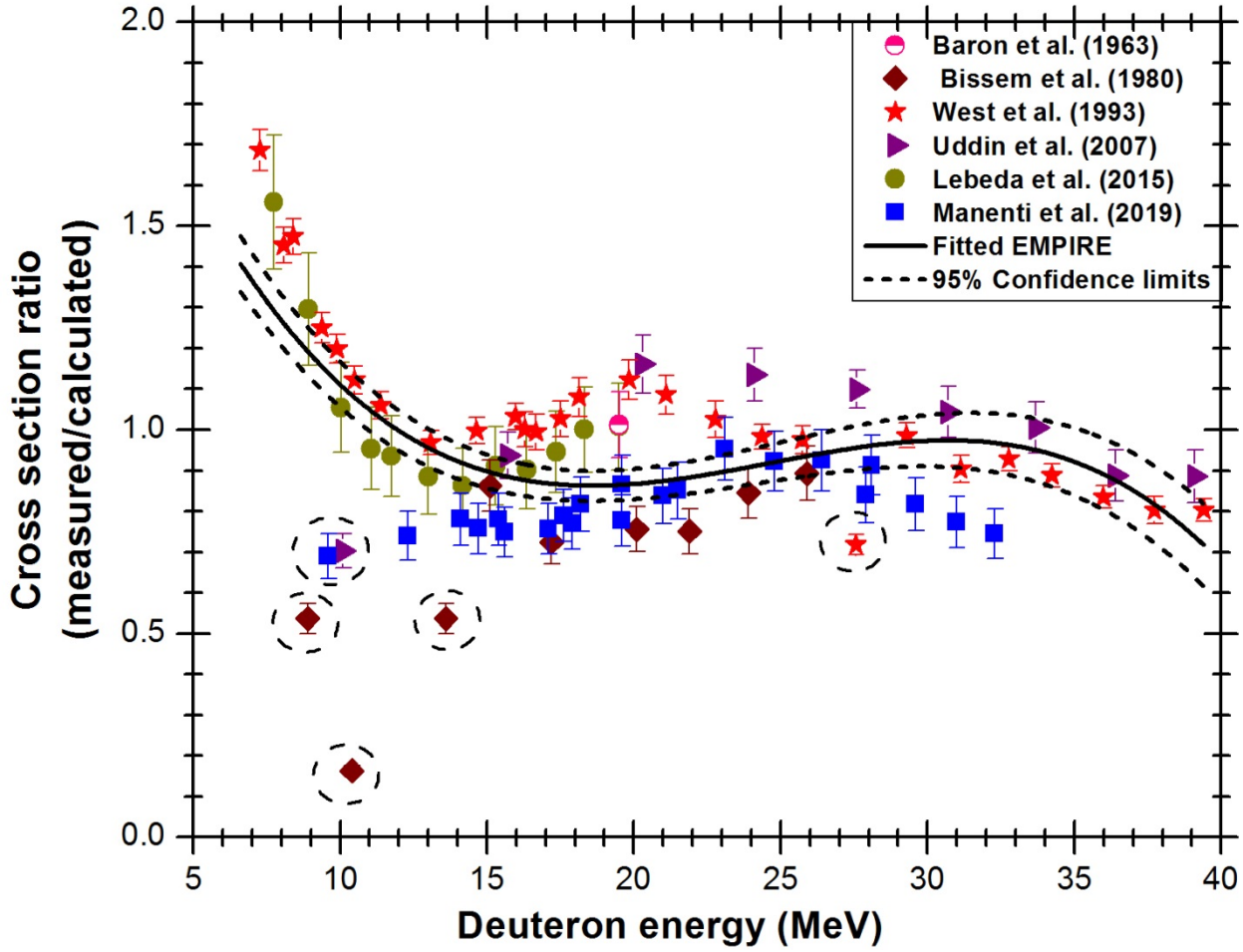
Baron et al. (1963)
Bissem et al. (1980)
West et al. (1993)
Uddin et al. (2007)
Lebeda et al. (2015)
Manenti et al. (2019)
Fitted EMPIRE
95% Confidence limits
Cross section ratio
(measured/calculated)
Deuteron energy (MeV)
2.0
1.5
1.0
0.5
0.0
5
10
15
20
25
30
35
40

Figure 3

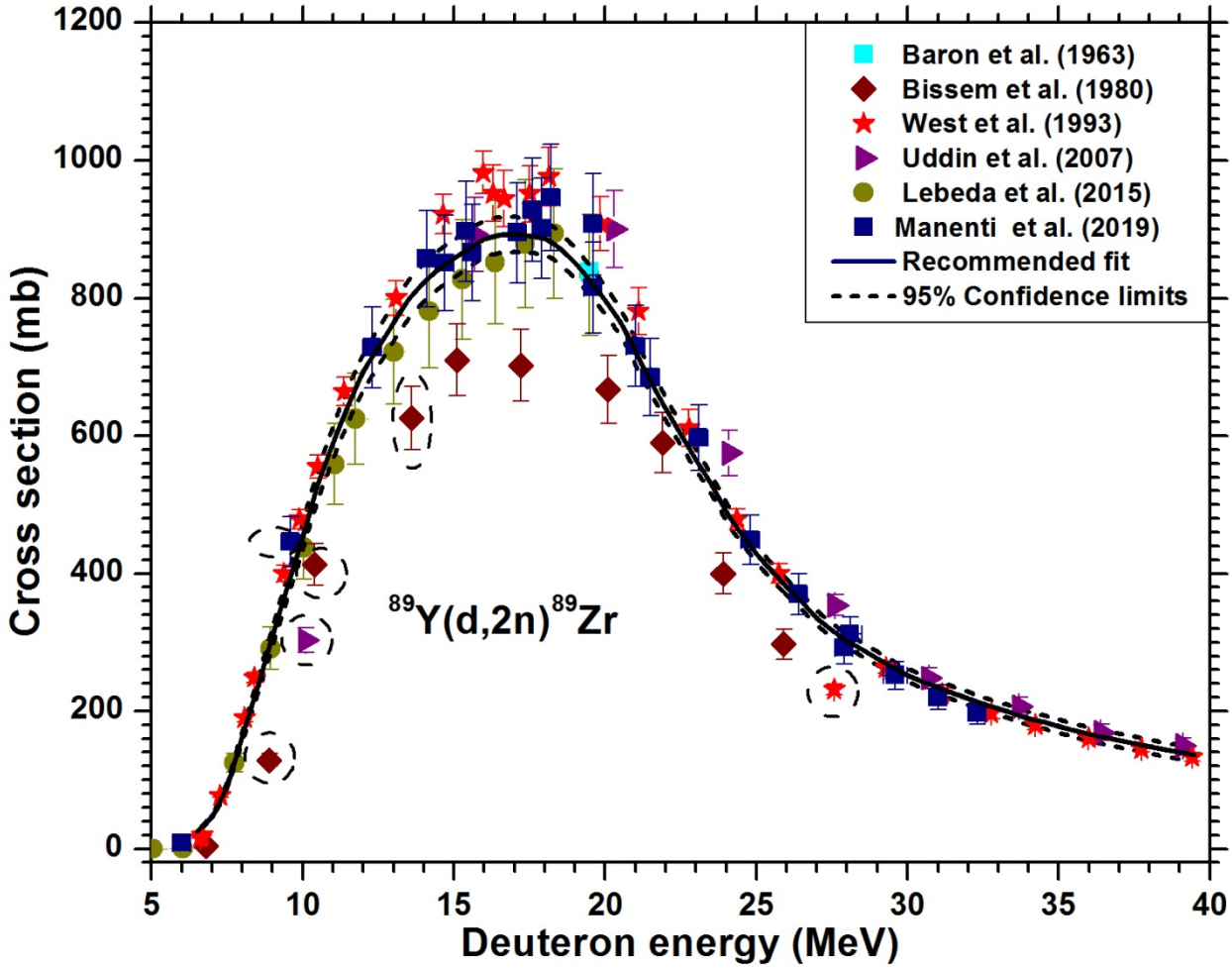
Baron et al. (1963)
Bissem et al. (1980)
West et al. (1993)
Uddin et al. (2007)
Lebeda et al. (2015)
Manenti et al. (2019)
Recommended fit
95% Confidence limits
89Y(d,2n)89Zr
Cross section (mb)
Deuteron energy (MeV)
0
200
400
600
800
1000
1200
5
10
15
20
25
30
35
40

Figure 4

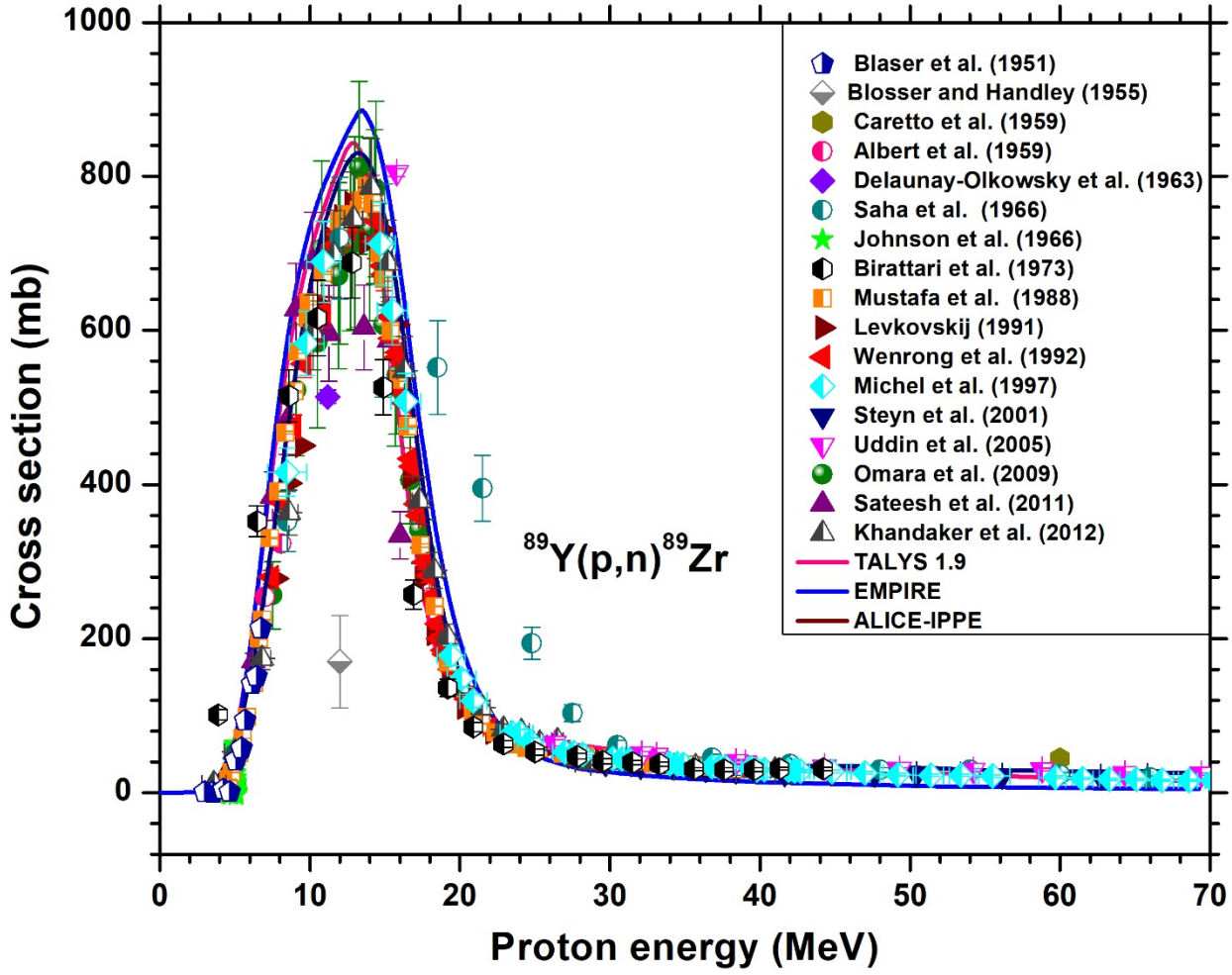
Cross section (mb)
Proton energy (MeV)
^{89}Y(p,n)^{89}Zr
Blaser et al. (1951)
Blosser and Handley (1955)
Caretto et al. (1959)
Albert et al. (1959)
Delaunay-Olkowsky et al. (1963)
Saha et al. (1966)
Johnson et al. (1966)
Birattari et al. (1973)
Mustafa et al. (1988)
Levkovskij (1991)
Wenrong et al. (1992)
Michel et al. (1997)
Steyn et al. (2001)
Uddin et al. (2005)
Omara et al. (2009)
Sateesh et al. (2011)
Khandaker et al. (2012)
TALYS 1.9
EMPIRE
ALICE-IPPE

Figure 5

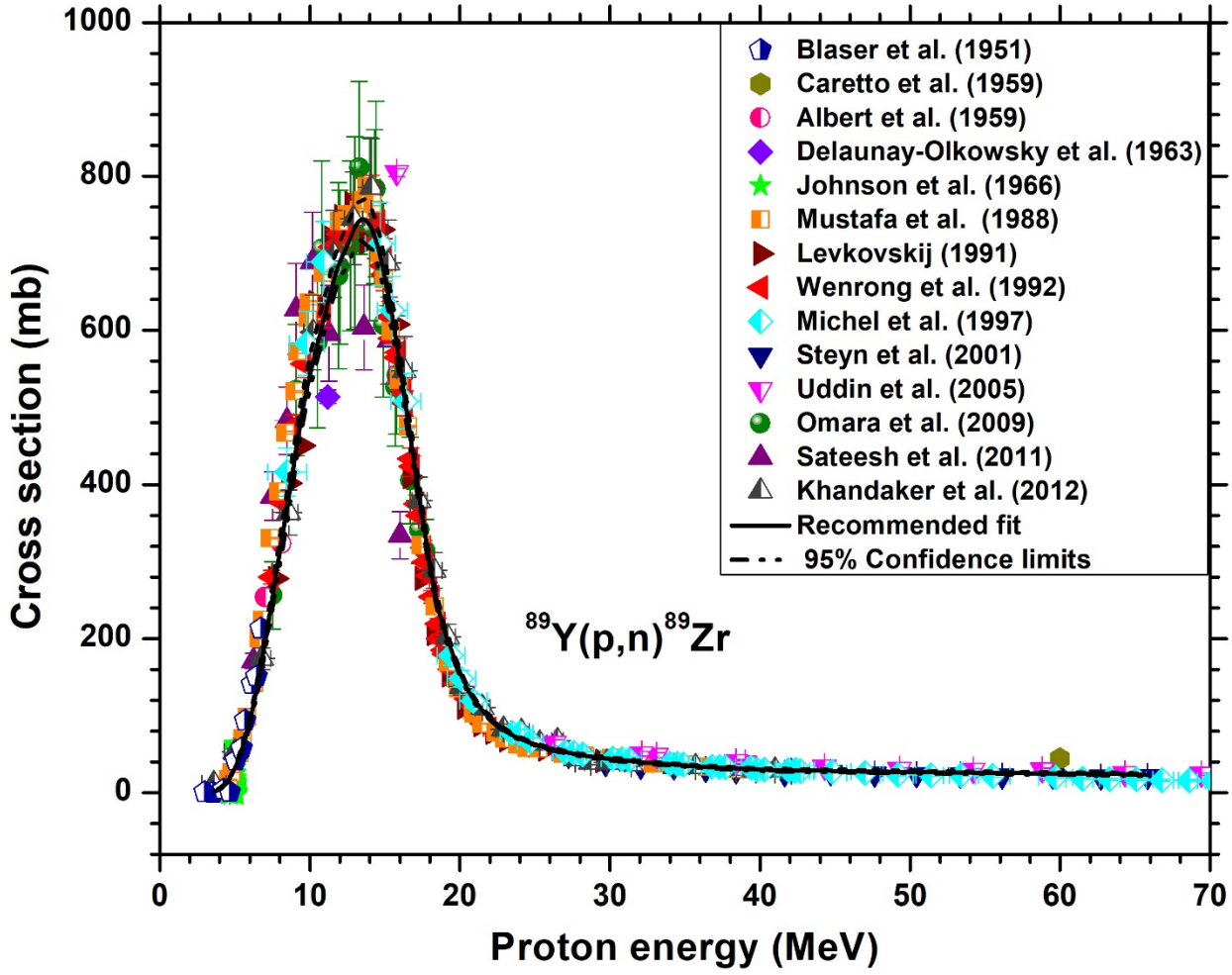
Cross section (mb)
Proton energy (MeV)
^{89}Y(p,n)^{89}Zr
Blaser et al. (1951)
Caretto et al. (1959)
Albert et al. (1959)
Delaunay-Olkowsky et al. (1963)
Johnson et al. (1966)
Mustafa et al. (1988)
Levkovskij (1991)
Wenrong et al. (1992)
Michel et al. (1997)
Steyn et al. (2001)
Uddin et al. (2005)
Omara et al. (2009)
Sateesh et al. (2011)
Khandaker et al. (2012)
Recommended fit
95% Confidence limits

Figure 6

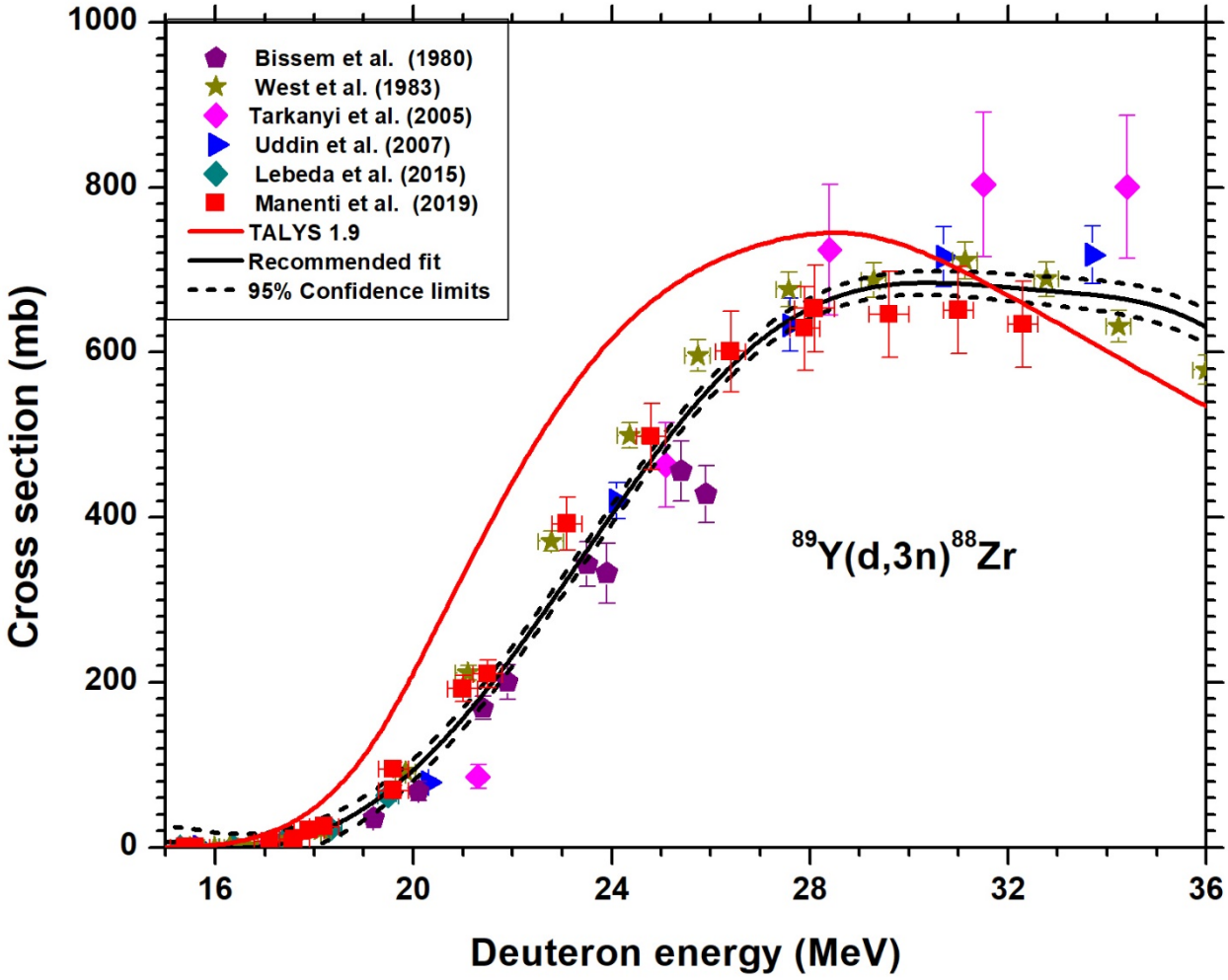
Bissem et al. (1980)
West et al. (1983)
Tarkanyi et al. (2005)
Uddin et al. (2007)
Lebeda et al. (2015)
Manenti et al. (2019)
TALYS 1.9
Recommended fit
95% Confidence limits
^{89}Y(d,3n)^{88}Zr
Cross section (mb)
Deuteron energy (MeV)
0
200
400
600
800
1000
16
20
24
28
32
36

Figure 7

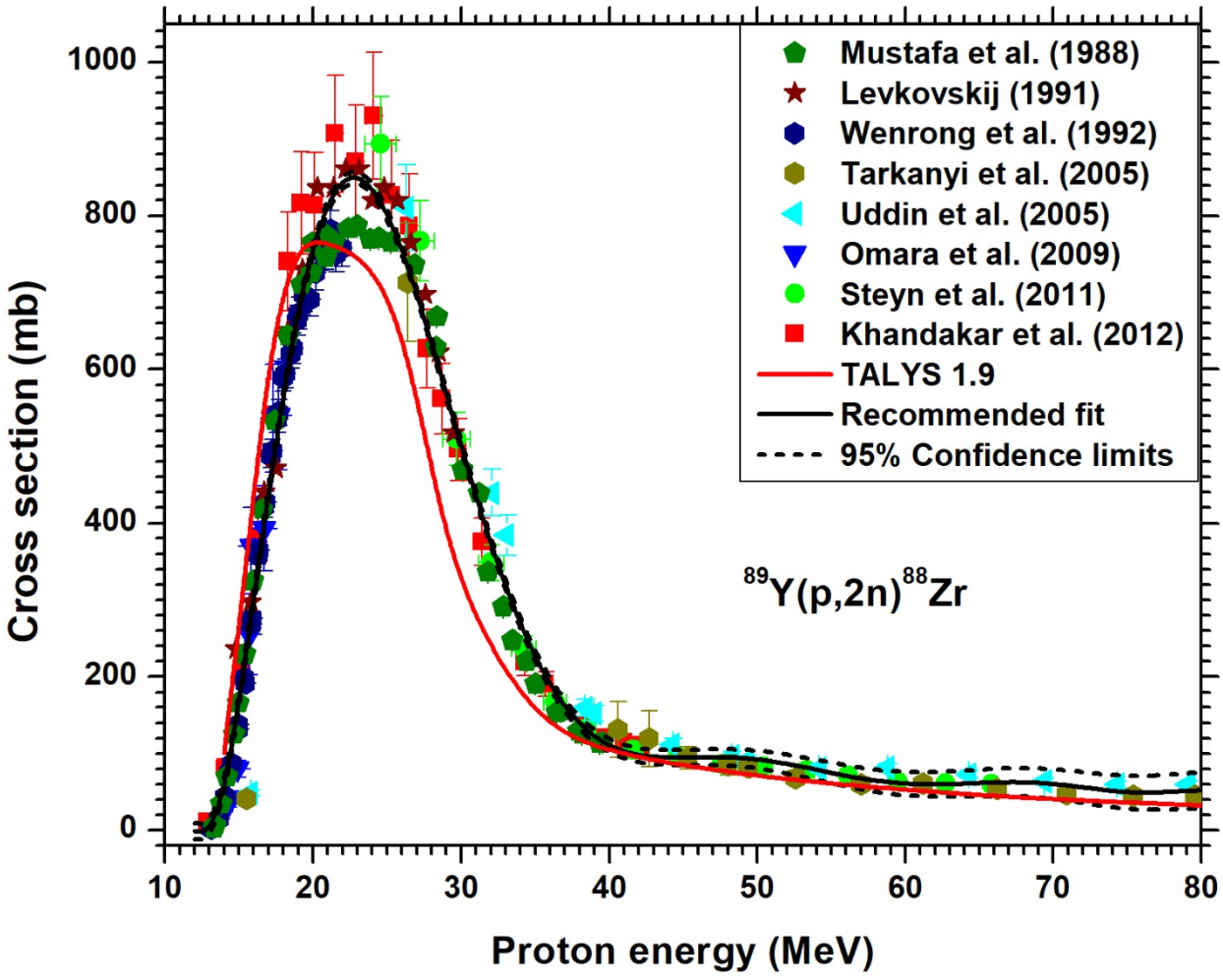
Mustafa et al. (1988)
Levkovskij (1991)
Wenrong et al. (1992)
Tarkanyi et al. (2005)
Uddin et al. (2005)
Omara et al. (2009)
Steyn et al. (2011)
Khandakar et al. (2012)
TALYS 1.9
Recommended fit
95% Confidence limits
89Y(p,2n)88Zr
Cross section (mb)
Proton energy (MeV)
0
200
400
600
800
1000
10
20
30
40
50
60
70
80

Figure 8

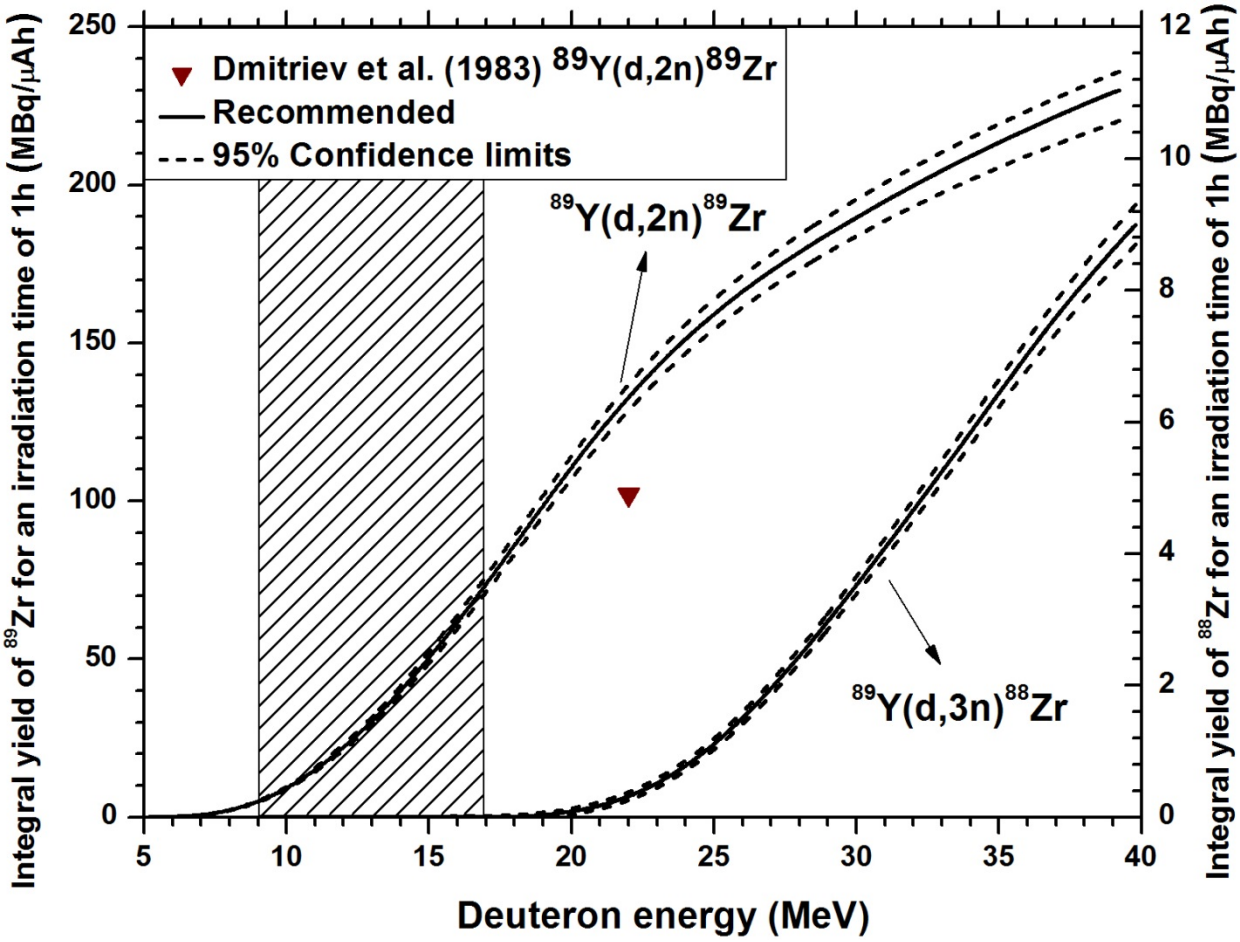
Dmitriev et al. (1983) 89Y(d,2n)89Zr
Recommended
95% Confidence limits
89Y(d,2n)89Zr
89Y(d,3n)88Zr
Integral yield of 89Zr for an irradiation time of 1h (MBq/μAh)
Integral yield of 88Zr for an irradiation time of 1h (MBq/μAh)
Deuteron energy (MeV)
0
50
100
150
200
250
0
2
4
6
8
10
12
5
10
15
20
25
30
35
40

Figure 9

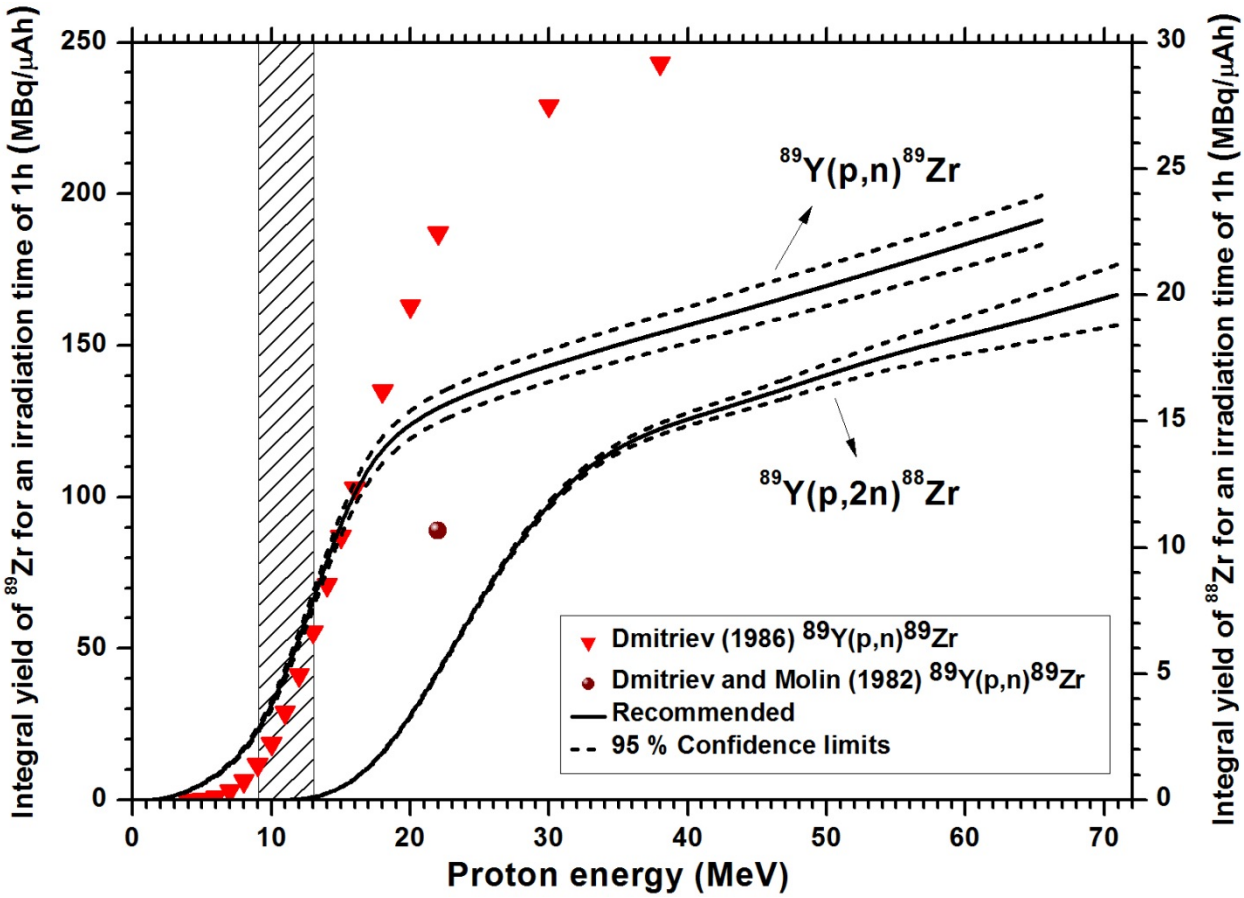
Integral yield of ^{89}Zr for an irradiation time of 1h (MBq/μAh)
Integral yield of ^{88}Zr for an irradiation time of 1h (MBq/μAh)
Proton energy (MeV)
^{89}Y(p,n)^{89}Zr
^{89}Y(p,2n)^{88}Zr
Dmitriev (1986) ^{89}Y(p,n)^{89}Zr
Dmitriev and Molin (1982) ^{89}Y(p,n)^{89}Zr
Recommended
95 % Confidence limits

Figure 10

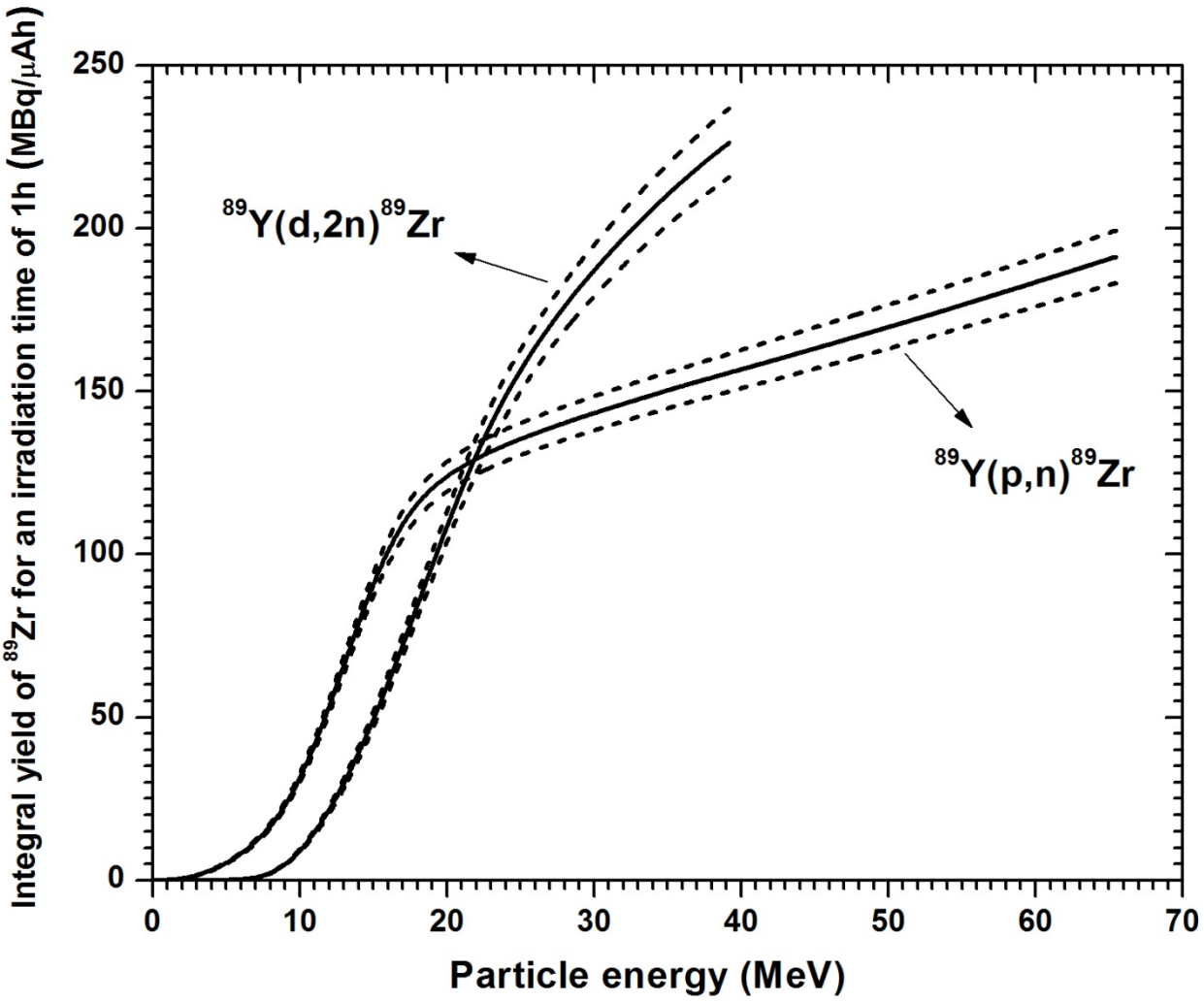
Integral yield of ^{89}Zr for an irradiation time of 1h (MBq/μAh)
Particle energy (MeV)
^{89}Y(d,2n)^{89}Zr
^{89}Y(p,n)^{89}Zr
0
50
100
150
200
250
0
10
20
30
40
50
60
70

Table 1 Decay Characteristics of of ^{89}Zr radionuclide*

Radionuclide	Decay Mode (%)	Half-life T1/2	gamma-ray Energy (keV)	Abundance(%) of γ-ray
^{89g}Zr	**β+ (100)**	78.41 h	**909.15**	**99**
^{89m}Zr	**β+ (6.2))** **EC (93.8)**	4.18 m	**587.8**	**89.62**

* taken from NuDat 2.7 (2019) (NuDat 2.7)

Table 2 Investigated nuclear reactions for the production of ^{89}Zr and major contributing radioactive impurity ^{88}Zr; with their Q values, threshold energies and references

Nuclear reaction	Q-Value (MeV)	Threshold energy (MeV)	References
^{89}Y(d,2n)^{89}Zr	-5.84	5.97	Baron et al., 1963; La Gamma et al, 1973; Bissem et al., 1980; Degering et al, 1988; West et al., 1993; Uddin, et al., 2007; Lebeda et al., 2015; Manenti et al., 2019
^{89}Y(d,3n)^{88}Zr	-15.2	15.5	Bissem et al., 1980; West et al., 1993; Tárkányi et al., 2005; Uddin et al., 2007; Lebeda et al., 2015; Manenti et al., 2019
^{89}Y(p,n)^{89}Zr	-3.62	3.66	Blaser et al., 1951; Blosser et al., 1955; Albert, 1959; Caretto et al., 1959; Delaunay-Olkowsky et al., 1963; Johnson et al., 1968; Birattari et al., 1973; Mustafa et al., 1988; Levkovskij, 1991; Wenrong et al., 1992; Saha et al., 1966; Michel et al., 1997; Uddin et al., 2005; Omara et al., 2009; Satheesh et al., 2011; Steyn et al., 2011; Khandaker et al., 2012;
^{89}Y(p,2n)^{88}Zr	-12.9	13.1	Mustafa et al., 1988; Levkovskij, 1991; Wenrong et al., 1992; Tárkányi et al., 2005; Uddin et al., 2005; Omara et al., 2009; Steyn et al., 2011; Khandaker et al., 2012

Table 3 Recommended cross sections for the $^{89}Y(d,2n)^{89}Zr$ reaction

Energy (MeV)	Cross section (mb)	95% confidence limits		Energy (MeV)	Cross section (mb)	95% confidence limits	
		Lower	Upper			Lower	Upper
6.5	25.1	23.8	26.4	21.5	679.9	662.6	697.3
7	46.0	43.7	48.3	22	639.8	586.7	656.2
7.5	91.6	87.1	96.2	22.5	602.4	572.2	632.5
9.5	382.0	365.0	398.0	23	565.7	550.8	580.6
10	453.1	434.0	472.3	23.5	530.7	516.4	544.9
10.5	529.4	507.6	551.1	24	489.4	476.0	502.8
11	589.7	566.1	613.4	24.5	457.9	445.1	470.8
11.5	644.7	619.5	670.0	25	428.7	416.5	441.0
12	693.6	667.2	720.0	25.5	403.6	391.8	415.5
12.5	728.6	701.6	755.7	26	380.4	368.9	391.8
13	765.1	737.5	792.6	26.5	359.7	348.6	370.8
13.5	798.1	770.1	826.0	27	335.1	324.5	345.7
14	823.2	795.2	851.2	27.5	317.5	307.2	327.9
14.5	842.3	814.5	870.1	28	302.2	292.1	312.4
15	857.3	829.9	884.8	28.5	289.4	279.4	299.4
15.5	872.6	845.5	899.7	29	276.5	266.7	286.4
16	885.6	858.9	912.2	29.5	263.7	254.0	273.3
16.5	891.6	865.6	917.7	30	252.0	242.5	261.6
17	893.0	867.6	918.4	31	234.5	225.0	244.0
17.5	890.4	865.7	915.0	32	218.4	208.9	227.9
18	886.4	862.4	910.4	33	203.5	194.0	213.1
18.5	872.3	849.2	895.5	34	189.1	179.6	198.7
19	851.8	829.6	874.0	35	178.0	168.4	187.7
19.5	825.7	804.4	846.9	36	166.4	156.7	176.2
20	797.6	777.2	817.9	37	157.3	147.4	167.1
20.5	765.6	746.1	785.0	38	148.4	138.5	158.3
21	721.9	703.6	740.3	39	140.2	130.3	150.0

Table 4 Recommended cross sections for the $^{89}Y(p,n)^{89}Zr$ reaction

Energy (MeV)	Cross section (mb)	95% confidence limits		Energy (MeV)	Cross section (mb)	95% confidence limits	
		Lower	Upper			Lower	Upper
4	4.1	3.7	4.5	21	118.5	115.0	122.0
4.5	13.0	11.9	14.1	21.5	107.0	103.8	110.2
5	30.4	28.1	32.7	22	96.8	93.9	99.7
5.5	55.7	51.7	59.7	22.5	88.2	85.6	90.8
6	93.3	87.1	99.5	23	80.1	77.8	82.5
6.5	137.9	129.3	146.4	23.5	74.6	72.3	76.8
7	191.3	180.0	202.5	24	70.3	68.1	72.4
7.5	253.0	238.9	267.2	24.5	66.3	64.3	68.4
8	313.2	296.6	329.8	25	62.2	60.3	64.2
8.5	370.6	351.9	389.2	26	57.1	55.3	59.0
9	430.7	410.0	451.4	27	52.9	51.1	54.6
9.5	486.9	464.6	509.3	28	48.9	47.2	50.6
10	532.6	509.1	556.0	29	46.0	44.3	47.6
10.5	570.6	546.5	594.8	30	43.6	42.0	45.3
11	607.5	582.7	632.3	31	41.7	40.1	43.3
11.5	645.5	620.1	671.0	32	39.6	38.0	41.2
12	680.8	654.9	706.7	33	38.2	36.5	39.8
12.5	709.1	682.9	735.3	34	36.9	35.2	38.5
13	736.5	710.0	763.0	35	35.3	33.7	36.9
13.5	745.6	719.4	771.8	36	33.9	32.3	35.5
14	737.9	712.5	763.3	37	32.7	31.1	34.3
14.5	712.8	688.7	736.9	38	31.8	30.2	33.4
15	670.7	648.4	693.0	39	30.8	29.2	32.4
15.5	619.6	599.2	639.9	40	30.0	28.4	31.5
16	555.3	537.3	573.4	42	29.0	27.4	30.6
16.5	488.0	472.4	503.7	44	28.4	26.8	30.0
17	422.2	408.7	435.6	46	27.8	26.2	29.5
17.5	359.5	348.2	370.8	48	27.2	25.6	28.9
18	291.7	282.5	300.8	50	26.7	25.1	28.4
18.5	244.0	236.4	251.6	55	25.6	24.0	27.3
19	208.8	202.4	215.3	60	24.8	23.1	26.4
19.5	181.1	175.6	186.6	65	23.5	21.9	25.2
20	156.6	151.8	161.3	66	22.9	21.2	24.5
20.5	133.4	129.4	137.4				

Table 5: Optimized energy ranges with thick target yield values of ^{89}Zr and percentage level of the radionuclidic impurity ^{88}Zr

Nuclear reaction	Energy range (MeV)	Thick target yield of ^{89}Zr* (MBq/μAh)	Radionuclidic impurity ^{88}Zr (%)
^{89}Y(d,2n)^{89}Zr	**17→7**	74	0
^{89}Y(d,2n)^{89}Zr	**30→17**	122	3
^{89}Y(p,n)^{89}Zr	**14→9**	63	0.36
^{89}Y(p,n)^{89}Zr	**13→9**	50.4	0

* Calculated from the recommended excitation function, assuming an irradiation time of 1 h at a beam current of 1 μA